Celebesides A–C and Theopapuamides B–D, Depsipeptides from an Indonesian Sponge That Inhibit HIV-1 Entry

ARTICLE *in* THE JOURNAL OF ORGANIC CHEMISTRY · JANUARY 2009

Impact Factor: 4.72 · DOI: 10.1021/jo802232u · Source: PubMed

Published in final edited form as:
J Org Chem. 2009 January 16; 74(2): 504–512. doi:10.1021/jo802232u.

Celebesides A-C and Theopapuamides B-D, Depsipeptides from an Indonesian Sponge that Inhibit HIV-1 Entry

Alberto Plaza[†], **Giuseppe Bifulco**[‡], **Jessica L. Keffer**[†], **John R. Lloyd**[†], **Heather L. Baker**[†], and **Carole A. Bewley**[†,*]

†*Laboratory of Bioorganic Chemistry, National Institute of Diabetes and Digestive and Kidney Diseases, National Institutes of Health, Bethesda, Maryland 20892-0820*

‡*Dipartimento di Scienze Farmaceutiche, University of Salerno, Via Ponte Don Melillo, 84084 Fisciano, Salerno, Italy*

Abstract

Six new depsipeptides belonging to two different structural classes, termed celebesides A-C and theopapuamides B-D, have been isolated from the marine sponge *Siliquariaspongia mirabilis*. Their structures were determined using extensive 2D NMR and ESI-MS/MS techniques. Celebesides are unusual cyclic depsipeptides that comprise a polyketide moiety and five amino acid residues, including an uncommon 3-carbamoyl threonine, and a phosphoserine residue in celebesides A and B. Theopapuamides B-D are undecapeptides with an N-terminal fatty acid moiety containing two previously unreported amino acids, 3-acetamido-2-aminopropanoic acid and 4-amino-2,3-dihydroxy-5-methylhexanoic acid. The relative configuration of the polyketide moiety in celebesides was resolved by *J*-based analysis and quantum mechanical calculations, the results of which were self consistent. Celebeside A neutralized HIV-1 in a single round infectivity assay with an IC_{50} value of 1.9 ± 0.4 μg/mL while the non-phosphorylated analog celebeside C was inactive at concentrations as high as 50 μg/mL. Theopapuamides A-C showed cytotoxicity against human colon carcinoma (HCT-116) cells with IC_{50} values between 2.1 and 4.0 μg/mL, and exhibited strong antifungal activity against wildtype and amphotericin B-resistant strains of *Candida albicans* at loads of 1-5 μg/disk.

Introduction

Lithistid demosponges are an abundant source of structurally diverse and biologically active natural products, which may be in part due to the biosynthetic capacity of the bacteria that they host.[1,2] In particular, marine sponges belonging to the Theonellidae family have yielded a number of unique compounds[2] with a broad spectrum of biological activities, including antifungal[3] and cancer cell growth inhibitors.[4,3d] Among this family, the chemistry of the genus *Siliquariaspongia* has been little studied.[5] Recently we reported the structures of a potent antitumor macrolide, mirabilin,[6] and several glycosylated depsipeptides, mirabamides A-D, that inhibit HIV-1 fusion,[7] from a *Siliquariaspongia mirabilis* sample collected in Chuuk. As part of our ongoing research on new bioactive natural products from marine organisms, we identified an aqueous extract of an Indonesian collection of *S. mirabilis* that showed activity in HIV-1 neutralization, antifungal and cytotoxicity assays. Bioassay-guided fractionation yielded a Sephadex fraction containing six new depsipeptides of two different structural classes, termed celebesides A-C (**1**-**3**), and theopapuamides B-D (**4**-**6**). The previously reported theopapuamide (**7**)[8] was also isolated from the same fraction. The structures of **1**-**6** were elucidated by extensive spectroscopic methods including 1D and 2D NMR experiments as well

*To whom correspondence should be addressed. Tel.: (301) 594-5187. Fax (301) 402-0008. E-mail: caroleb@mail.nih.gov.

as ESI-MS analysis. The absoluteconfigurations of the amino acids were determined by LCMS (advanced Marfey's method)[9] and chiral HPLC. The relative configurations of chiral centers of the polyketide residues were established by combined analysis of homonuclear (H-H) and heteronuclear (C-H) $^{2,3}J$ couplings, ROE data, and quantum mechanical calculations.

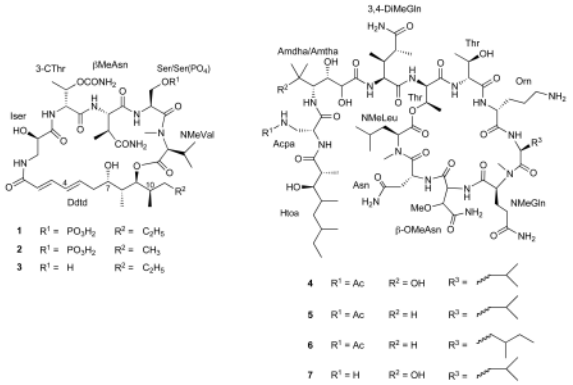

Results and Discussion

The HR-ESI-MS of celebeside A (**1**) showed a major ion peak at *m/z* 892.4054 $[M+H]^+$ corresponding to a molecular formula of $C_{37}H_{62}N_7O_{16}P$ (calcd for $C_{37}H_{63}N_7O_{16}P$, 892.40689) and suggesting the presence of a phosphate group. The ^1H NMR spectrum of **1** exhibited signals characteristic of a peptide containing a polyketide section including six exchangeable NH protons from δ 6.68 to 8.14; one methyl amide at δ 3.05 (3H, s); six methyl doublets at δ 0.74 (3H, d, *J* = 6.6 Hz), 0.794 (3H, d, *J* = 7.0 Hz), 0.796 (3H, d, *J* = 6.0 Hz), 0.93 (3H, d, *J* = 6.4 Hz), 1.10 (3H, d, *J* = 7.1 Hz), and 1.17 (3H, d, *J* = 6.4 Hz); and one methyl triplet at δ 0.82 (3H, t, *J* = 7.1 Hz). Signals corresponding to four olefinic protons at δ 6.00 (1H, d, *J* = 15.5 Hz), 6.05 (1H, dd, *J* = 15.3, 6.6), 6.23 (1H, dd, *J* = 15.3, 11.1 Hz), and 7.06 (1H, dd, *J* = 15.5, 11.1 Hz) were present in the downfield region of the spectrum. The HSQC spectrum clearly showed that the four methines from δ 4.47 to 4.92 and the methylene at δ 3.55 and 3.41 were correlated to five carbons at δ 43.9 to 63.0, indicating the presence of five amino acid residues (see Table 1). This evidence in combination with the DQF-COSY, 2D-HOHAHA, and HMBC correlations allowed us to establish the presence of *N*-methylvaline (*N*MeVal), serine, β-methylasparagine (βMeAsn), threonine, and isoserine (Iser). The downfield chemical shift of the threonine β-oxymethine proton at δ 5.01 and its HMBC correlation to a carbonyl resonance at δ 157.8 indicated an ester linkage of the threonine residue to a carbamic acid.[10] In similar fashion, phosphorylation of the serine residue (pSer) was deduced from the down field chemical shifts observed for the β-oxymethylene of serine (δ_H 3.85 and 3.95, δ_C 65.2) in the HSQC spectrum. Furthermore, these results were corroborated by ESI-MS/MS analysis. The daughter ion spectrum of the major ion at *m/z* 914 $[M+Na]^+$ displayed fragment ions at *m/z* 853 $[M+Na-61]^+$ and *m/z* 816 $[M+Na-98]^+$ corresponding to the neutral loss of a carbamic acid residue and a phosphate group, respectively. To our knowledge, this is the first occurrence of a 3-carbamoyl threonine (3-CThr) or a phosphorylated serine residue in a marine natural product.

The structure of the polyketide residue was deduced as follows. A conjugated diene spin system (δ_{H-2} 6.00, δ_{C-2} 123.5, δ_{H-3} 7.06, δ_{C-3} 141.6, δ_{H-4} 6.23, δ_{C-4} 131.4, δ_{H-5} 6.05, δ_{C-5} 140.2) assigned from HSQC-TOCSY and COSY correlations was linked to a carbonyl group by HMBC correlations from the H-2 and H-3 protons to the carbon resonance at δ_C 169.5 (C-1). HSQC-TOCSY and COSY correlations extended the diene spin system to a sequential allylic methylene (δ_{H-6} 2.34, 2.20, δ_{C-6} 38.6), an oxymethine (δ_{H-7} 3.33, δ_{C-7} 70.6), a methine (δ_{H-8} 1.70, δ_{C-8} 38.5), and additional oxymethine group (δ_{H-9} 5.00, δ_{C-9} 78.7). Finally, key long

range correlations from the methyl protons at δ 0.794 (Me-8) to the carbon resonances at δ 70.6, 38.5, and 78.7; from the methyl protons at δ 0.796 (Me-10) to the carbon resonances at δ 78.7, 34.3 (C-10), and 37.5 (C-11); and from the secondary methyl at δ 0.82 (Me-13) to the carbon resonances at δ 21.0 and 37.5 allowed complete assembly of the polyketide residue. On the basis of this information the structure of the polyketide residue was established as 7,9-dihydroxy-8,10-dimethyltrideca-2,4-dienoic acid (Ddtd).

The complete sequence of **1** was obtained from HMBC and ROESY correlations. Long-range correlations between α-protons to carbonyl carbons of adjacent amino acids and ROE correlations from α-protons to NH protons of adjacent amino acids allowed us to establish the following sequence: Iser–3-CThr–βMeAsn–pSer–*N*MeVal (see Table 1). Moreover, connectivity of the Ddtd unit to the N-terminus of Iser was indicated from an HMBC correlation between the Iser α-methylene protons (δ 3.55 and 3.41) and the carbonyl at δ 169.5 (C-1_{Ddtd}). Finally, the downfield chemical shift of the Ddtd oxymethine proton at δ 5.00 (H-9_{Ddtd}) suggested an ester linkage at this position, which was confirmed by an HMBC correlation between H-9_{Ddtd} and the carbonyl carbon of *N*MeVal (δ 171.3), thereby completing the structure of **1** as a 26-membered ring. Tandem mass spectrometry provided further evidence to support the structure of **1**. MS^3 fragmentation of the daughter ion at *m/z* 853 $[M+Na\text{-}NH_2CO_2H]^+$ displayed fragment ions at *m/z* 755 $[M+Na\text{-}NH_2CO_2H\text{-}H_3PO_4]^+$, and *m/z* 740 $[M+Na\text{-}NH_2CO_2H\text{-}N\text{MeVal}]^+$. Successively, MS^4 fragmentation of the ion peak at *m/z* 755 gave fragments at *m/z* 642 $[M+Na\text{-}NH_2CO_2H\text{-}H_3PO_4\text{-}N\text{MeVal}]^+$, *m/z* 573 [M+Na-*N*MeVal-Pser]$^+$, and *m/z* 390 $[M+Na\text{-}NH_2CO_2H\text{-}H_3PO_4\text{-}N\text{MeVal-Ddtd}]^+$. Thus, the MS^n fragmentation patterns were in complete agreement with the structure of **1** determined by NMR.

The absolute configurations of L-*N*MeVal, L-Ser, D-3-CThr, and D-Iser residues were assigned by MS–detected chromatographic comparison of the acid hydrolysate (5 N HCl, 90 °C, 16 h) of **1** with L-FDLA (1-fluoro-2,4-dinitrophenyl-5-L-leucinamide)[9] and D-FDLA derivatives of amino acid standards. The absolute configuration of βMeAsn was also established by this method owing to the report by Fujii, *et al*.[9a] that the L-FDLA derivative of βMeAsn elutes before the D-FDLA derivative. As detected by LC-MS (reconstructed ion chromatogram, *m/z* 440 $[M-H]^-$), L/D-FDLA derivatives of βMeAsn of **1** eluted at 20.9 and 22.1 min while the L-FDLA derivative eluted at 20.9 min, thus establishing the configuration of βMeAsn as L. To distinguish between *erythro* and *threo* configurations, L-FDLA and D-FDLA derivatives of βMeAsn in **1** and in an authentic sample of microcystin LR, shown by X-ray crystallography to contain *erythro*-D-βMeAsn,[11] were compared. LC-MS analysis showed the D-FDLA derivative of **1** to coelute with the L-FDLA derivative of microcystin; thus celebeside A must contain *erythro*-L-βMeAsn. Further confirmation of the *erythro* configuration was provided from Murata's *J*-based configurational analysis.[12] The combination of a medium vicinal coupling constant between H-$3_{\beta MeAsn}$ and H-$2_{\beta MeAsn}$ (5.5 Hz), a small $^3J_{H\text{-}C}$ for H-$2_{\beta MeAsn}$/$\beta Me_{\beta MeAsn}$ (2.2 Hz), and a medium $^2J_{H\text{-}C}$ for H-$3_{\beta MeAsn}$/C-$2_{\beta MeAsn}$ (-3.0 Hz) is indicative of an *erythro* (2*S*, 3*R*) configuration at C-2/C-3.

Several techniques were used to establish the configurations of the Ddtd unit. The *E* geometries of the $\Delta^{2\text{-}3}$ and $\Delta^{4\text{-}5}$ olefins were apparent from the large $^3J_{H\text{-}H}$ values of 15.5 and 15.3 Hz between H-2_{Ddtd}/H-3_{Ddtd} and H-4_{Ddtd}/H-5_{Ddtd}, respectively. The relative configurations of the chiral centers at C-7, C-8, C-9, and C-10 in Ddtd were determined by a combination of *J*-based configurational analysis,[12] and quantum mechanical calculations of the homonuclear and heteronuclear *J*-coupling values. Experimental data including $^3J_{H\text{-}H}$ (^{1}H NMR and E.COSY[13]) and $^{2,3}J_{C\text{-}H}$ couplings, and ROEs were compared to those predicted for all possible staggered rotamers (Figure 1). Due to the complex multiplicity and small homonuclear coupling constants of the methine protons H-8_{Ddtd} and H-10_{Ddtd}, heteronuclear coupling constants were accurately measured from 2D NMR experiments including HETLOC,[14] HSQMBC,[15] and constant time *J*-resolved HMBC[16] experiments; and ROE correlations were

obtained from ROESY and HSQC-ROESY[17] experiments. All experiments were recorded on samples dissolved in a mixture of 5:1 CD_3CN–D_2O at 298 K. A small $^3J_{H\text{-}H}$ of 1.0 Hz between H-7_{Ddtd} and H-8_{Ddtd} indicated a gauche configuration between these protons, and a small heteronuclear $^3J_{C\text{-}H}$ of 3.1 Hz indicated a gauche configuration between H-7_{Ddtd} and C-9_{Ddtd}. Together these values rule out models **A1**, **A2**, **A4**, and **A6** (Figure 1a). Additionally, respective $^3J_{C\text{-}H}$ values of 2.6 and 5.5 Hz for H-8_{Ddtd}/C-6_{Ddtd} and H-7_{Ddtd}/Me-8_{Ddtd} excluded rotamer **A5** indicating the correct conformation to be that depicted in **A3**. Strong ROEs between H-7_{Ddtd} and H-8_{Ddtd}, H-7_{Ddtd} and H-9_{Ddtd}, and H-6_{Ddtd} and Me-8_{Ddtd} corroborated this result and established a *syn* configuration for C-7_{Ddtd} and C-8_{Ddtd}. The *anti* configuration between Me-8_{Ddtd} and the hydroxyl group at C-9_{Ddtd}, corresponding to rotamer **B4**, was deduced from the large coupling constant between H-8_{Ddtd} and H-9_{Ddtd} (10.6 Hz) and strong HSQC-ROESY correlations between Me-8_{Ddtd} and H-10_{Ddtd} and Me-8_{Ddtd} and H-9_{Ddtd} (Figure 1b). The small $^3J_{H\text{-}H}$ of 1.1 Hz between H-9_{Ddtd} and H-10_{Ddtd} (Figure 1c) indicated a gauche configuration between these protons, while a small heteronuclear coupling of $^2J_{H10\text{-}C9}$ = 1.3 Hz obtained from the G-BIRD-HSQMBC spectrum indicated an anti orientation between H-10_{Ddtd} and the hydroxyl group at C-9_{Ddtd}. Taken together, these data rule out rotamers **C2**–**C5** (Figure 1c). The relatively large $^3J_{Me10\text{-}H9}$ value of 5.3 Hz suggested an anti configuration between H-9_{Ddtd} and Me-10_{Ddtd}, and further excluded model **C6**. Therefore, the relative configuration for C-9_{Ddtd}/C-10_{Ddtd} was established as *anti*. This result was supported by ROE correlations between H-9_{Ddtd} and H-10_{Ddtd} and H-9_{Ddtd} and H-11_{Ddtd}, and a strong HSQC-ROESY correlation between H-8_{Ddtd} and Me-10_{Ddtd}. On the basis of the results obtained by using Murata's method, the relative configuration of the chiral centers in Ddtd was established as 7*S**, 8*R**, 9*S**, and 10*R**.

Strictly speaking, the NMR *J*-based analysis is applicable to staggered rotamers within acyclic carbon chains.[18] As Ddtd is located within a macrocycle, we sought to corroborate the relative configuration of its chiral centers by using an integrated NMR–quantum mechanical approach that relies on the comparison between calculated and experimental $^3J_{H\text{-}H}$ and $^{2,3}J_{C\text{-}H}$ values.[19] This approach is particularly appropriate in cases where experimentally determined coupling constants fall between the ranges qualitatively classified as ‘large’ or ‘small’. While the ^{1}H resolution and relatively large range (0 to 12 Hz) of homonuclear 3-bond coupling constants facilitates reliable assignment of $^3J_{H\text{-}H}$ values as large or small, the reduced resolution in the ^{13}C dimension together with the smaller spread (0 to 6 Hz) of $^{2,3}J_{C\text{-}H}$ values makes even qualitative classification of long-range heteronuclear coupling constants more difficult and less reliable. As an example, experimental $^3J_{C\text{-}H}$ values for H-7/C-9, H-8/C-6, and H-9/C-11 within the Ddtd portion of **1** were found to be 3.1, 2.6, and 4.0 Hz, respectively, all of which may be classified as ‘medium’. To quantitatively compare experimental with predicted couplings surrounding these centers, we performed quantum mechanical calculations at the DFT MPW1PW91/6-31G(d,p) level of *J* values for all possible configurations in the simplifed fragment **8** (represented by the stereoisomers shown in projections A1-A6, B1-B6, and C1-C6 in Figure 1). The results are summarized in Table 2 where the calculated values for the six possible conformers (three *threo* and three *erythro* arrangements) for stereocenter pairs C-7/C-8, C-8/C-9, and C-9/C-10 are presented alongside their experimental values (far right column). Total Absolute Deviation (TAD) values, which provide an unbiased measure of the similarity between calculated and experimental coupling constants for each isomer, are shown in italics. Isomers displaying the lowest TAD values include A3 for C-7/C-8 (5.5 Hz), B4 for C-8/C-9 (5.5 Hz), and C1 for C-9/C10 (4.2 Hz). These calculated values correspond to 7*S**, 8*R**, 9*S**, and 10*R** configurations, confirming the *J*-based assignments presented above. It is noteworthy that, in addition to these configurations being self-consistent among stereocenter pairs, the results of the *J* coupling quantum chemical analysis are perfectly compatible with the experimental ROESY correlations (Figure 2).

Residues similar to Ddtd have been found in the antibacterial depsipeptide nagahamide A[21] and the antifungal antibiotic YM-47522.[22] In both compounds the relative configuration of the polyketide residue was established as 7*R**, 8*R**, 9*S**, and 10*R**, while the absolute configuration of YM-47522 was established as 7S, 8S, 9R, and 10S by synthesis of its enantiomer.[23] In keeping with the different relative configurations at C-7 in celebeside A (*7S**) and nagahamide (*7R**), it is noteworthy that the ^{13}C chemical shifts for $Me10_{Ddtd}$ in DMSO-d_6 differ significantly with respective δ_C values of 12.9 and 16.8.

The HR-ESI-MS of celebeside B (**2**) showed a major ion peak at *m/z* 878.3964 $[M+H]^+$ ($C_{37}H_{60}N_7O_{16}P$, calcd for $C_{36}H_{61}N_7O_{16}P$, 878.3912), fourteen mass units lower than that of **1**. The 2D NMR data for **2** closely resembled those of **1** with the exception that resonances belonging to the polyketide residue Ddtd were replaced by resonances belonging to a 7,9-dihydroxy-8,10-dimethyldodeca-2,4-dienoic acid (Dddd) residue. HR-ESI-MS data gave a molecular formula $C_{37}H_{61}N_7O_{13}$ (*m/z* 812.4443 $[M+H]^+$, calcd for $C_{37}H_{62}N_7O_{13}$, 812.4406) for celebeside C **(3**), 80 mass units below that of **1**. Analysis of the NMR data (^1H, ^{13}C, HSQC, HMBC, DQF-COSY, 2D-HOHAHA) established **3** to be the dephosphorylated analogue of **1**. LC-MS analysis of the L/D-FDLA-derivatized hydrolysates of **2** and **3** revealed all amino acid residues to possess configurations identical to those in **1**. Additionally, analysis of the NMR data corresponding to signals belonging to the polyketide unit indicated that the configurations in **2** and **3** are the same as those in **1**.

Evident from the mass spectral data, Sephadex fractions containing the celebesides also contained a suite of compounds with considerably higher masses. The molecular formula of **4** was established as $C_{71}H_{125}N_{17}O_{24}$ on the basis of HR-ESI-MS (*m/z* 800.9600 $[M+2H]^{2+}$, calcd for $C_{71}H_{125}N_{17}O_{24}$, 1599.9083). Its NMR spectrum displayed characteristic signals of a peptide, including resonances attributable to exchangeable amide protons between δ 9.16 and 6.20, α-amino protons between δ 5.12 and 3.90, two methyl amide signals at δ 2.82 (3H, s) and 2.86 (3H, s), and one ester carbinol proton at δ 5.12 (1H, d, *J* = 3.6 Hz). Additionally, the ^1H NMR spectrum showed signals corresponding to a methoxyl at δ 3.34 (3H, s), an acetamide methyl at δ 1.90 (3H, s), and a primary methyl at δ 0.83 (3H, t, *J* = 7.3 Hz). A detailed analysis of the 2D NMR data established the presence of one equivalent each of *N*-methylleucine (*N*MeLeu), asparagine, β-methoxyasparagine (β-OMeAsn), *N*-methylglutamine (*N*MeGlu), leucine, ornithine, 3,4-dimethylglutamine (3,4-DiMeGln), 3-hydroxy-2,4,6-trimethyloctanoic acid (Htoa), and two threonine residues, one of which was *O*-acylated. The presence of an unusual 3-acetamido-2-aminopropanoic acid (Acpa) was established by HMBC correlations from the β-aminomethylene protons at δ 3.54 and 3.49 to the acetamide carbonyl at δ 174.9. The presence of 4-amino-2,3,5-trihydroxy-5-methylhexanoic acid (Amtha) was deduced as follows. A contiguous spin system comprising two oxymethine signals (δ_H 3.75, δ_C 71.8 and δ_H 4.06, δ_C 71.5) and one aminomethine signal (δ_H 3.97, δ_C 56.1) was apparent from HSQC, COSY and TOCSY spectra. HMBC correlations from the oxymethine proton at δ 3.75 to the carbonyl resonance at δ 176.9 ($C\text{-}1_{Amtha}$); and from the methyl protons at δ 1.24 ($Me\text{-}6_{Amtha}$) and 1.09 ($Me\text{-}5_{Amtha}$), and the aminomethine proton at δ 3.97, to the oxygenated quaternary carbon at 74.9 ($C\text{-}4_{Amtha}$) secured the structure of this residue.

Long-range correlations between α-protons and carbonyl carbons of adjacent amino acids provided the sequence (in the direction CO to N) *N*MeLeu–Asn–β-OMeAsn–*N*MeGlu–Leu–Orn–Thr1–Thr2–3,4-DiMeGln–Amtha for **4**, with the hydroxyl group of Thr2 forming an ester bond with the carboxyl group of *N*MeLeu. The remainder of the sequence was deduced from HMBC spectra. In particular, long range correlations between the aminomethine proton $H\text{-}4_{Amtha}$ and the carbonyl resonance at δ 173.1 ($C\text{-}1_{Acpa}$) linked Acpa to the main fragment, while an HMBC correlation between the α-proton at δ 4.49 ($H\text{-}2_{Acpa}$) and the carbonyl resonance at δ 179.4 ($C\text{-}1_{Htoa}$), linked the fatty acid Htoa to Acpa. This sequence was further corroborated by analysis of the MS/MS spectrum. Fragmentation of the doubly charged ion

peak at *m/z* 801 $[M+2H]^{+2}$ displayed fragment ions at *m/z* 1271 $[M+H\text{-Htoa-Acpa-}NH_3]^+$, *m/z* 957 [M+H-Htoa-Acpa-Amtha-3,4-DiMeGln]$^+$, *m/z* 754 [M+H-Htoa-Acpa-Amtha-3,4-DiMeGln-Thr-Thr]$^+$, and *m/z* 627 [M+H-Htoa-Acpa-Amtha-3,4-DiMeGln-Thr-Thr-*N*MeLeu]$^+$, consistent with the sequence established for **4**.

The absolute configurations of L-*N*MeLeu, L-*N*MeGln, L-Leu, D-Orn, D-allo-Thr, and D-Acpa were assigned by chromatographic comparison of the acid hydrolysate of **4** (5 N HCl, 90 °C, 16 h) with appropriate amino acid standards after derivatizing with L/D-FDLA (1-fluoro-2,4-dinitrophenyl-5-L/D-leucinamide).[9] Comparison by LC-MS of the L/D-FDLA derivative of 3,4-DiMeGln of **4** with that derivative from the hydrolysate of an authentic sample of mirabamide A[7] showed that DiMeGln has the same configuration, (3*S*,4*R*)-dimethyl-L-glutamine, in both peptides. Chiral HPLC following acid hydrolysis of **4** established the D configuration for Asn.

The HR-ESI-MS of **5** and **6** showed doubly charged ion peaks at *m/z* 792.9615 $[M + 2H]^{2+}$ and *m/z* 799.9722 $[M+2H]^{2+}$ corresponding to molecular formulae of $C_{71}H_{125}N_{17}O_{23}$ (calcd for $C_{71}H_{125}N_{17}O_{23}$, 1583.9134) and $C_{72}H_{127}N_{17}O_{23}$ (calcd for $C_{72}H_{127}N_{17}O_{23}$, 1597.9291), respectively. These values indicated that the molecular weight of **5** was 16 mu lower than **4** while **6** was 14 mu higher than **5**. A detailed analysis of the NMR data of **5** clearly established that its amino acid sequence was identical to **4**, except for the occurrence of a 4-amino-2,3-dihydroxy-5-methylhexanoic acid (Amdha) residue instead of Amtha. Similarly, the 2D NMR data of **6** differed to that of **5** by the substitution of an uncommon homoisoleucine (hIle) residue for a leucine residue. Once again, LC-MS analysis of the L/D-FDLA-derivatized hydrolysates of **5** and **6** revealed that all the amino acid residues possessed identical configurations to that in **4**, and the configuration of hIle was established as L.

On the basis of the amino acid sequences of **4**-**6**, it was evident that these depsipeptides resembled theopapuamide (**7**), previously isolated from an extract of *T. swinhoei* Gray collected in Papua New Guinea, and reported to be cytotoxic.[8] However, the configuration of the chiral centers in the polyketide residues in theopapuamide were not reported.

In theopapuamide B (**4**), the relative configurations of the chiral centers C-3/C-4 in Amtha, and C-2/C-3 in Htoa were solved using again *J*-based configuration analysis in the following manner. A large $^3J_{H\text{-}H}$ of 9.1 Hz obtained from the phase-sensitive COSY-35 spectrum[24] indicated an anti orientation between protons H-2_{Htoa} and H-3_{Htoa} (Figure 3a). The *anti* configuration between Me-2_{Htoa} and the hydroxyl group at C-3_{Htoa} was assigned on the basis of ROESY correlations between Me-2_{Htoa}/H-4_{Htoa}, Me-2_{Htoa}/H-3_{Htoa}, and H-2_{Htoa}/H-4_{Htoa}. The configuration at C-3_{Htoa}/C-4_{Htoa}, however, could not be solved using the *J*-based analysis because of alternation between conformers.[13] This situation was apparent from the small $^3J_{H\text{-}H}$ between H-3_{Htoa} and H-4_{Htoa} (2.3 Hz), and intermediate $^3J_{C\text{-}H}$ values of 4.6 and 4.5 Hz between H-3_{Htoa} and C-5_{Htoa}, and H-3_{Htoa} and Me-4_{Htoa}, respectively, indicating alternation between g+ and g- conformers at C-3/C-4. Recently, Zampella *et al.* reported the structure of homophymine, a cyclic depsipeptide that also contains an exocyclic Htoa residue (referred to in that paper as HTMOA).[25] In the case of homophymine, the authors did not report conformational averaging around C-3/C-4, and through the combined use of *J*-based, NOE and Mosher's analysis, were able to assign a 2*R*,3*R*,4*R*,6*R* configuration for that residue.

Within the Amtha residue, a small $^3J_{H\text{-}H}$ (<1 Hz) between H-3_{Amtha} and H-4_{Amtha} suggested a gauche orientation between these two protons (Figure 3b). Moreover, the constant time *J*-resolved HMBC spectrum showed large $^2J_{C\text{-}H}$ coupling constants of 5.1 Hz and 4.7 Hz between H-4_{Amtha} and C-3_{Amtha} and between H-3_{Amtha} and C-4_{Amtha}, respectively. Together these values indicated a *syn* configuration at C-3_{Amtha}/C-4_{Amtha}. Within the β-OMeAsn residue, however, alternation between g+ and g- conformers at C-2/C-3, apparent from small $^3J_{H\text{-}H}$ and intermediate $^2J_{C\text{-}H}$ values, precluded our ability to use these methods to establish its relative

stereochemistry. Last, analysis of the NMR data of the polyketide residues Htoa and Amdha in theopapuamides C and D suggested identical relative configurations to those observed for theopapuamide B.

Celebesides A and C and theopapuamides A-C were evaluated in a single round HIV-1 infectivity assay[26,27] against viruses pseudotyped with HIV-1 SF162 Envelope, and a cytotoxicity assay using human colon tumor cell line HCT-116. The results are summarized in Table 3. Interestingly, celebeside A inhibits HIV-1 Entry with an IC_{50} value of 1.9±0.4 μg/mL, while the non-phosphorylated celebeside C was inactive at concentrations as high as 50 μg/mL. Theopapuamide B (**4**) was active in the neutralization assay with an IC_{50} value of 0.8 ± 0.3 μg/mL; however, we found theopapuamides A-C to be cytotoxic to other healthy cell lines at similar concentrations (data not shown). Celebeside A and theopapuamides A-C were also cytotoxic to a human colon tumor cell line (HCT-116) with IC_{50} values of 8.8, 2.1, 4.0 and 2.1 μg/mL, respectively.

The antifungal activity of the crude extract was traced to the theopapuamides, and testing of pure compounds **4**, **5** and **7** revealed activity against both wild type and amphotericin B-resistant strains of *Candida albicans*. In particular, theopapuamide A inhibited growth of wild type and amphotericin B-resistant strains at loadings of 1 μg/disk, displaying zones of growth inhibition of 8 mm; and theopapuamides B and C were slightly less potent, displaying zones of inhibition of 10 mm at 5 μg/disk against both strains. All three celebesides were found to be inactive toward *Bacillus subtilis*, *Escherichia coli*, *Pseudomonas aeruginosa*, *Staphylococcus aureus* and *Candida albicans* at concentrations as high as 50 μg/disk.

In summary, we have isolated six new depsipeptides from an *S. mirabilis* sponge collected from Indonesia. Celebesides A-C (**1**-**3**) are cyclic depsipeptides that contain the polyketide moiety Ddtd and five amino acid residues, among which are the unusual amino acids phosphoserine and 3-carbamoyl threonine, both of which are new to marine natural products. Interestingly, the anti-HIV activity of celebesides correlates with the presence of phosphoserine. The undecapeptides theopapuamides B-D (**4**-**6**) are further members of the theopapuamide class reported recently by Ireland and coworkers. Theopapuamides C and D contain two new entities, including 3-acetamido-2-aminopropanoic acid and 4-amino-2,3-dihydroxy-5-methylhexanoic acid, while theopapuamide D contains a rare homoisoleucine residue. Theopapuamides A-C showed strong antifungal activity toward amphotericin B-resistant *C. albicans* and its parent strain. Thus, celebesides and theopapuamides represent interesting new classes of anti-infectives. In addition to these six new depsipeptides, aurantosides A and B[28] and keramamide A[29] were also found in the aqueous extract of this sponge. The presence of this suite of compounds in a single collection of *S. mirabilis* further emphasizes the chemical diversity present in lithistid demosponges.

Experimental Section

General Experimental Procedures

Optical rotations were measured with a Jasco P-2000 polarimeter, IR spectra were recorded on a Perkin Elmer FT-IR Spectrum One spectrometer, and UV spectra were recorded on an Agilent 8453 spectrophotometer. NMR spectra were recorded in 5:1 or 4:1 CD_3CN-H_2O on a Bruker DRX-600 spectrometer (^1H at 600 MHz, ^{13}C at 150 MHz). DQF-COSY, 2D-HOHAHA, HSQC, HMBC, and ROESY experiments were recorded using standard pulse programs all of which included water suppression (Watergate). HSQC experiments were optimized for $^1J_{C\text{-}H}$ = 145 Hz, and HMBC spectra were optimized for $^{2,3}J_{C\text{-}H}$ = 8 and 5 Hz. The accurate mass electrospray ionization (ESI) mass spectra were measured on a Waters LCT Premier time-of-flight (TOF) mass spectrometer. The instrument was operated in W-mode at a nominal resolution of 10,000. The electrospray capillary voltage was set at 2KV and the

sample cone voltage at 60 volts. The desolvation temperature was set to 275 °C and nitrogen was used as the desolvation gas with a flow rate of 300 L/hr. Accurate masses were obtained using the internal reference standard method. MS/MS data were obtained using a Thermo-Scientific (San Jose, CA, USA) LTQ ion Trap mass spectrometer. Sample was infused into the mass spectrometer using an Advion BioSciences (Ithaca, NY, USA) Triversa chip based nano-electrospray ionization system. The nitrogen gas pressure was 0.25 PSI and the electrospray tip voltage was 1.4KV. The CID MS/MS collision energy was 35Vand the parent ion isolation width was 3 Daltons. The maximum injection time for parent ions was 700 ms and 500 ms for daughter ions. The maximum AGC ion target setting was 1 × 10e5 for parent ions and 5 × 10e4 for daughter ions.

Computational Details

For the quantum mechanical calculations, both full geometry optimization and calculation of *J*-coupling values were performed using the Gaussian03 (version B.05) software package.[20] The *gauche* or *anti* staggered conformers of a simplified fragment, **8**, containing 14 carbon atoms were optimised at mPW1PW91 level of theory using the 6-31G(d,p) basis set; the single-point calculation of *J*-coupling was executed on the optimized geometries using the same mPW1PW91 functional and the 6-31G(d,p) basis set.

Sponge Material

Samples of *S. mirabilis* (deLaubenfels, 1954) (lithistid Demospongiae: family Theonellidae) were collected around Sulawesi Island, Indonesia, at a depth of 43 m in 1994. The sample was identified as described previously,[6] and a voucher specimen has been deposited at the Natural History Museum, London, United Kingdom (BMNH 2007.7.9.1). Samples were frozen immediately after collection, and shipped frozen to Frederick, MD, where they were freeze-dried and extracted with H_2O.

Isolation

A 6 g portion of the extract was partitioned between *n*-BuOH-H_2O (1:1) to afford a dried *n*-BuOH extract (0.7 g) that was fractionated on a Sephadex LH-20 column (50 × 2.5 cm) eluting with MeOH:H_2O (7:3). Fractions containing peptides were combined and dried in vacuo to give 130 mg that were subsequently purified by reverse-phase HPLC (Jupiter Proteo C12, 250 × 10 mm, 4μ, DAD at 220 and 280 nm) eluting with a linear gradient of 50–80% MeOH in 0.05% TFA in 50 min to afford compounds **1** (7.2 mg, t_R = 43.9 min), **2** (2.4 mg, t_R = 34.9 min), **3** (1.1 mg, t_R = 40.0 min), **4** (2.5 mg, t_R = 32.9 min), **5** (1.8 mg, t_R = 33.5 min), **6** (0.8 mg, t_R = 36.8 min), and **7** (3.4 mg, t_R = 24.3 min).

Celebeside A (1): colorless amorphous powder; $[\alpha]^{23}_{D}$ -49.9 (*c* 0.32, MeOH); IR (film) ν_{max} 3333, 1665, 1534, 1201, 1139, 1076 cm^{-1}; UV (MeOH) λ_{max} (log ε) 210 (2.98), 270 (2.17) nm; ^1H and ^{13}C NMR data, see Table 1; HR-ESI-MS *m/z* 892.4054 $[M + H]^+$ corresponding to a molecular formula of $C_{37}H_{62}N_7O_{16}P$ (calcd for $C_{37}H_{63}N_7O_{16}P$, 892.40689).

Celebeside B (2): colorless amorphous powder; $[\alpha]^{23}_{D}$ -2.0 (*c* 0.05, MeOH); IR (film) ν_{max} 3330, 1663, 1538, 1207, 1132, 1075 cm^{-1}; UV (MeOH) λ_{max} (log ε) 210 (2.96), 271 (2.15) nm; ^1H and ^{13}C NMR data for Iser, Thr, βMeAsn, pSer, and *N*MeVal are identical to those reported for **1** in Table 1; ^1H NMR (CD_3CN-H_2O 5:1, 600 MHz) Dddd: δ 6.02 (1H, d, *J* = 15.5 Hz, H-2), 7.05 (1H, dd, *J* = 15.5, 11.1 Hz, H-3), 6.25 (1H, dd, *J* = 15.3, 11.1 Hz, H-4), 6.01 (1H, dd, *J* = 15.3, 6.6 Hz, H-5), 2.40 (1H, td, *J* = 13.9, 6.6 Hz, H-6a), 2.22 (1H, td, *J* = 13.9, 6.5 Hz, H-6b), 3.36 (1H, t, *J* = 7.4 Hz, H-7), 1.70 (1H, m, H-8), 5.04 (1H, dd, *J* = 10.6 1.1 Hz, H-9), 1.64 (1H, m, H-10), 1.25 (1H, m, H-11a), 1.11 (1H, m, H-11b), 0.87 (3H, t, *J* = 7.0 Hz, Me-12), 0.78 (3H, d, *J* = 7.0 Hz, Me-8), 0.79 (3H, d, *J* = 6.3 Hz, Me-10); ^{13}C NMR (CD_3CN-H_2O 5:1, 150 MHz) Dddd: δ 169.5 (C-1), 123.5 (C-2), 141.6 (C-3), 131.8 (C-4), 140.3 (C-5),

39.0 (C-6), 70.6 (C-7), 38.5 (C-8), 78.6 (C-9), 37.0 (C-10), 28.2 (C-11), 12.4 (Me-12), 9.3 (Me-8), 13.0 (Me-10); HR-ESI-MS *m/z* 878.3964 $[M+H]^+$ ($C_{37}H_{60}N_7O_{16}P$, calcd for $C_{36}H_{61}N_7O_{16}P$, 878.3912).

Celebeside C (3): colorless amorphous powder; $[\alpha]^{23}_D$ -3.4 (*c* 0.06, MeOH); IR (film) ν_{max} 3420, 1676, 1192, 1130 cm^{-1}; UV (MeOH); λ_{max} (log ε) 211 (2.98), 272 (2.17) nm; ^1H and ^{13}C NMR data for Iser, Thr, βMeAsn, *N*MeVal, and Ddtd are identical those reported for **1** in Table 1; ^1H NMR (CD_3CN-H_2O 5:1, 600 MHz) Ser: δ 4.78 (1H, m, H-2), 3.54 (1H, m, H-3a), 3.50 (1H, m, H-3b), 7.61 (1H, br, NH); ^{13}C NMR (CD_3CN-H_2O 5:1, 150 MHz) Ser: δ 171.2 (C-1), 53.3 (C-2); HR-ESI-MS *m/z* 812.4443 $[M+H]^+$ ($C_{37}H_{61}N_7O_{13}$, calcd for $C_{37}H_{62}N_7O_{13}$, 812.4406)

Theopapuamide B (4): colorless amorphous powder; $[\alpha]^{23}_D$ 7.1 (*c* 0.1, MeOH); IR (film) ν_{max} 3329, 1673, 1536, 1205, 1185, 1138 cm^{-1}; UV (MeOH) λ_{max} (log ε) 210 (3.84) nm; HR-ESI-MS *m/z* 800.9600 $[M+2H]^{2+}$, (calcd for $C_{71}H_{125}N_{17}O_{24}$, 1599.9083). See Supporting Information for ^1H and ^{13}C NMR assignments.

Theopapuamide C (5): colorless amorphous powder; $[\alpha]^{23}_D$ 5.1 (*c* 0.08, MeOH); IR (film) ν_{max} 3319, 1673, 1534, 1203, 1181, 1134 cm^{-1}; UV (MeOH) λ_{max} (log ε) 210 (3.83) nm; HR-ESI-MS *m/z* 792.9615 $[M + 2H]^{2+}$, (calcd for $C_{71}H_{125}N_{17}O_{23}$, 1583.9134). See Supporting Information for ^1H and ^{13}C NMR assignments.

Theopapuamide D (6): colorless amorphous powder; $[\alpha]^{23}_D$ 2.5 (*c* 0.03, MeOH); IR (film) ν_{max} 3325, 1675, 1532, 1208, 1185, 1139 cm^{-1}; UV (MeOH) λ_{max} (log ε) 210 (3.84) nm; HR-ESI-MS *m/z* 799.9722 $[M + 2H]^{2+}$, (calcd for $C_{72}H_{127}N_{17}O_{23}$, 1597.9291). See Supporting Information for ^1H and ^{13}C NMR assignments.

Theopapuamide A (7): colorless amorphous powder; $[\alpha]^{23}_D$ 6.4 (*c* 0.2, MeOH); HR-ESI-MS *m/z* 779.9548 $[M + 2H]^{2+}$, (calcd for $C_{69}H_{123}N_{17}O_{23}$, 1557.8978).

LC/MS Analysis of L/D-FDLA Derivatives

Approximately 0.5 mg of compounds **1**-**6** were separately hydrolyzed with 5 N HCl (LabChem Inc, traceable to NIST) (0.8 mL) in an Ace high pressure tube for 16 h at 90 °C, dried, and dissolved in H_2O (100 μL). To a 50 μL aliquot of each was added 1 N $NaHCO_3$ (20 μL) and 1% 1-fluoro-2,4-dinitrophenyl-5-L-leucinamide (L -FDLA or D-FDLA solution in acetone, 100 μL), and the mixtures were heated to 40 °C for 40 min, allowed to cool to rt, neutralized with 2 N HCl (20 μL), and evaporated to dryness. Residues were dissolved in CH_3CN and analyzed by LC-MS. Analyses of the L- and L/D-FDLA (mixture of D- and L-FDLA) derivatives were performed using a Phenomenex Jupiter Proteo C12 column (4 μm, 150 × 4.6 mm). Aqueous CH_3CN containing 0.01 M TFA was used as a mobile phase eluting with a linear gradient of 25-70% CH_3CN in 45 min at a flow rate of 0.5 mL/min. An Agilent Series 1100 MSD mass spectrometer was used for detection in negative ESI mode. The fragmentor and capillary voltage were kept at 70 and 1000 V, respectively, and the ion source at 350 °C. A mass range of *m*/*z* 100-1000 was scanned in 0.1 min. Retention times (t_R, min) of the FDLA-derivatized amino acids for compounds **1**-**3**: L-Iser 19.9, D-Iser 19.3 *m/z* 398 $[M-H]^-$; L-*N*MeVal 29.7, D-*N*MeVal 33.2 *m/z* 424 $[M-H]^-$; L-Thr 19.3, D-Thr 23.2 *m/z* 412 $[M-H]^-$; erythro-L-βMeAsn 20.8, erythro-D-βMeAsn 24.1 *m/z* 440 $[M-H]^-$. Retention times (t_R, min) of the FDLA-derivatized amino acids for compounds **4**-**6**: L-*N*MeLeu 33.5, D-*N*MeLeu 35.5 *m/z* 438 $[M-H]^-$; L-*N*MeGln 19.7, D-*N*MeGln 21.0 *m/z* 426 $[M-H]^-$; L-Leu 30.6, D-Leu 36.6 *m/z* 424 $[M-H]^-$; L-Orn 36.8, D-Orn 34.8 *m/z* 720 $[M-H]^-$ (bis derivative); L-*allo*Thr 20.5, D-*allo*Thr 21.8 *m/z* 412 $[M-H]^-$; (3*S*,4*R*)-dimethyl-L-glutamine 23.3, (3*S*,4*R*)-dimethyl-D-glutamine 24.3 *m/z* 467 $[M-H]^-$; L-Dpa 37.5, D-Dpa 38.0 *m/z* 692 $[M-H]^-$ (bis derivative);L-hIle 30.1, D-hIle 39.3 *m/z* 438 $[M-H]^-$.

Chiral HPLC analysis

The acid hydrosylates of **3**-**6** (0.3 mg) were analyzed by chiral HPLC on a Phenomenex column [Chirex Phase 3126 (D) 150 × 4.6 mm] eluting with 1 mM CuSO4:MeCN (95:5) at a flow rate of 0.5 mL/min, with UV detection at 254. The retention times of Asp were compared to authentic standards whose retention times were 15.5 min for L-Asp and 19.9 min for D-Asp.

Biological assays

Cytotoxicity assays were carried out using an MTT cell proliferation assay kit (American Type Culture Collection) according to the instructions provided. Briefly, HCT-116 or TZM-BL cells were seeded in 96-well tissue culture plates at a density of 2×10^4 cells/well in 50 μl of growth media and allowed to adhere for 18 hr. Attached cells were incubated with inhibitors for 24 hr (as controls for the neutralization assay), after which the media was either replaced or diluted 3-fold with fresh growth media. Following an additional 48 h incubation period, cell viability was assessed upon treatment with MTT (A_{570}, Molecular Devices 96-well absorbance plate reader). Single round HIV-1 neutralization assays were performed with viruses pseudotyped with SF162 Envelope using published conditions.[26]

Antimicrobial activity

Compounds **1**-**6** were tested for antimicrobial activity against *Pseudomonas aeruginosa* (ATCC 15442), *Escherichia coli* (ATCC 8739), *Staphylococcus aureus* (ATCC 25923), *Bacillus subtilis* (ATCC 49343), and wild type (ATCC 90027) and amphotericin B resistant *C. albicans* (ATCC 200955) using a modified disk diffusion assay. Agar plates seeded with suspensions of bacteria or fungi were prepared by adding 500 μL of a 24 h culture of bacteria to 100 mL of autoclaved Antibiotic Medium 2 (AB2) containing 1% agar and cooled to 55 °C, or of fungi to Sabouraud Dextrose Agar (SDA) at 55°C. Seeded liquid agar (10 mL) was transferred immediately to square Petri dishes and allowed to cool for 1 h. Control drugs used for each microorganism included kanamycin (50 μg) for *P. aeruginosa* and *S. aureus*, ampicillin (50 μg) for *E. coli*, choloroamphenicol (10 μg) for *B. subtilis*, and amphotericin B (25 μg) for *C. albicans*. Following incubation at 37°C for 18 h, zones of inhibition resulting from antibiotics or depsipeptides (1-50 μg) were measured.

Supplementary Material

Refer to Web version on PubMed Central for supplementary material.

Acknowledgements

We thank the Coral Reef Research Foundation, D. Newman and the country of Indonesia for making possible sample acquisition; M. Kelly and the National Cancer Institute for sponge taxonomy; L. Bell, CRRF, for helpful discussions; and the AIDS Research and Reference Reagent Program, Division of AIDS, NIAID, NIH, for reagents and cell lines used in the HIV-1 neutralization assays. This work was supported in part by the NIH Intramural Research Program (NIDDK) and the Intramural AIDS Targeted Antiviral Program, Office of the Director, NIH (C.A.B.).

References

1. Bewley CA, Faulkner DJ. Angew Chem Int Ed Engl 1998;37:2162.
2. Matsunaga S, Fusetani N. Curr Org Chem 2003;7:945.
3. (a) Matsunaga S, Fusetani N, Kato Y, Hirota H. J Am Chem Soc 1991;113:9690. (b) Matsunaga S, Fusetani N, Hashimoto K, Walchli M. J Am Chem Soc 1989;111:2582. (c) Bewley CA, Faulkner DJ. J Org Chem 1994;59:4849. (d) Youssef DTA, Mooberry SL. J Nat Prod 2006;69:154. [PubMed: 16441091]
4. (a) Kashman Y, Carmely S. Tetrahedron Lett 1985;26:511. (b) Kobayashi M, Tanaka J, Katori T, Matsuura M, Kitagawa I. Tetrahedron Lett 1989;22:2963. (c) Kitagawa I, Kobayashi M, Katori T,

Yamashita M, Tanaka J, Doi M, Ishida T. J Am Chem Soc 1990;112:3710. (d) Doi M, Ishida T, Kobayashi M, Kitagawa I. J Org Chem 1991;56:3629. (e) Hamada T, Matsunaga S, Yano G, Fusetani N. J Am Chem Soc 2005;127:110. [PubMed: 15631460]

5. (a) Sata NU, Matsunaga S, Fusetani N, van Soest RWM. J Nat Prod 1999;62:969. [PubMed: 10425118] (b) Sata NU, Wada SI, Matsunaga S, Watabe S, van Soest RWM, Fusetani N. J Org Chem 1999;64:2331.
6. Plaza A, Baker HL, Bewley CA. J Nat Prod 2008;71:473. [PubMed: 18271553]
7. Plaza A, Gustchina E, Baker HL, Kelly M, Bewley CA. J Nat Prod 2007;70:1753. [PubMed: 17963357]
8. Ratnayake AS, Bugni TS, Feng X, Harper MK, Skalicky JJ, Mohammed KA, Andjelic CD, Barrows LR, Ireland CM. J Nat Prod 2006;69:1582. [PubMed: 17125225]
9. (a) Fujii K, Ikai Y, Oka H, Suzuki M, Harada KI. Anal Chem 1997;69:5146. (b) Fujii K, Ikai Y, Mayumi T, Oka H, Suzuki M, Harada KI. Anal Chem 1997;69:3346.
10. Bui HTN, Jansen R, Pham HTL, Mundt S. J Nat Prod 2007;70:499. [PubMed: 17311455]
11. Goldberg J, Huang HB, Kwon YG, Greengard P, Nairn AC, Kuriyan J. Nature 1995;376:745. [PubMed: 7651533]
12. Matsumori N, Kaneno D, Murata M, Nakamura H, Tachibana K. J Org Chem 1999;64:866. [PubMed: 11674159]
13. Griesinger C, Sorensen OW, Ernst RR. J Magn Reson 1987;75:474.
14. Uhrin D, Batta G, Hruby VJ, Barlow PN, Koever KE. J Magn Reson 1998;130:155. [PubMed: 9515088]
15. (a) Marquez BL, Gerwick WH, Williamson RT. Magn Reson Chem 2001;39:499. (b) Williamson RT, Marquez BL, Gerwick WH, Kover KE. Magn Reson Chem 2000;38:265.
16. Meissner A, Soerensen OW. Magn Reson Chem 2001;39:49.
17. Bax A, Davis DG. J Magn Reson 1985;63:207.
18. Bifulco G, Dambruoso P, Gomez-Paloma L, Riccio R. Chem Rev 2007;107:3744. [PubMed: 17649982]
19. Bifulco G, Bassarello C, Riccio R, Gomez Paloma L. Org Lett 2004;6:1025–1028. [PubMed: 15012091]
20. Frisch, MJ.; Trucks, GW.; Schlegel, HB.; Scuseria, GE.; Robb, MA.; Cheeseman, JR.; Montgomery, JA., Jr; Vreven, T.; Kudin, KN.; Burant, JC.; Millam, JM.; Iyengar, SS.; Tomasi, J.; Barone, V.; Mennucci, B.; Cossi, M.; Scalmani, G.; Rega, N.; Petersson, GA.; Nakatsuji, H.; Hada, M.; Ehara, M.; Toyota, K.; Fukuda, R.; Hasegawa, J.; Ishida, M.; Nakajima, T.; Honda, Y.; Kitao, O.; Nakai, H.; Klene, M.; Li, X.; Knox, JE.; Hratchian, HP.; Cross, JB.; Bakken, V.; Adamo, C.; Jaramillo, J.; Gomperts, R.; Stratmann, RE.; Yazyev, O.; Austin, AJ.; Cammi, R.; Pomelli, C.; Ochterski, JW.; Ayala, PY.; Morokuma, K.; Voth, GA.; Salvador, P.; Dannenberg, JJ.; Zakrzewski, VG.; Dapprich, S.; Daniels, AD.; Strain, MC.; Farkas, O.; Malick, DK.; Rabuck, AD.; Raghavachari, K.; Foresman, JB.; Ortiz, JV.; Cui, Q.; Baboul, AG.; Clifford, S.; Cioslowski, J.; Stefanov, BB.; Liu, G.; Liashenko, A.; Piskorz, P.; Komaromi, I.; Martin, RL.; Fox, DJ.; Keith, T.; Al Laham, MA.; Peng, CY.; Nanayakkara, A.; Challacombe, M.; Gill, PMW.; Johnson, B.; Chen, W.; Wong, MW.; Gonzalez, C.; Pople, JA. Gaussian 03, Revision B.05. Gaussian Inc.; Wallingford CT: 2004.
21. Okada Y, Matsunaga S, van Soest RWM, Fusetani N. Org Lett 2002;4:3029.
22. (a) Shibazaki M, Sugawara T, Nagai K, Shimizu Y, Yamaguchi H, Suzuki K. J Antibiot 1996;49:340. [PubMed: 8641995] (b) Sugawara T, Shibazaki M, Nakahara H, Suzuki K. J Antibiot 1996;49:345. [PubMed: 8641996]
23. Ermolenko MS. Tetrahedron Lett 1996;37:6711.
24. Bax A, Freeman R. J Magn Reson 1981;44:542.
25. Zampella A, Sepe V, Luciano P, Bellotta F, Monti MC, D'Auria MV, Jepsen T, Petek S, Adeline MT, Laprévôte O, Aubertin AM, Debitus C, Poupat C, Ahond A. J Org Chem 2008;73:5319. [PubMed: 18563935]
26. Li M, Gao F, Mascola JR, Stamatatos L, Polonis VR, Koutsoukos M, Voss G, Goepfert P, Gilbert P, Greene KM, Bilska M, Kothe DL, Salazar-Gonzalez JF, Wei X, Decker JM, Hahn BH, Montefiori DC. J Virol 2005;79:10108. [PubMed: 16051804]
27. Gustchina E, Bewley CA, Clore GM. J Virol. 2008in press; PMID 18667502

28. Matsunaga S, Fusetani N, Kato Y. J Am Chem Soc 1991;113:9690–9692.
29. Kobayashi J, Sato M, Ishibashi M, Shigemori H, Nakamura T, Ohizumi Y. J Chem Soc Perkin Trans I 1991:1050–1052.

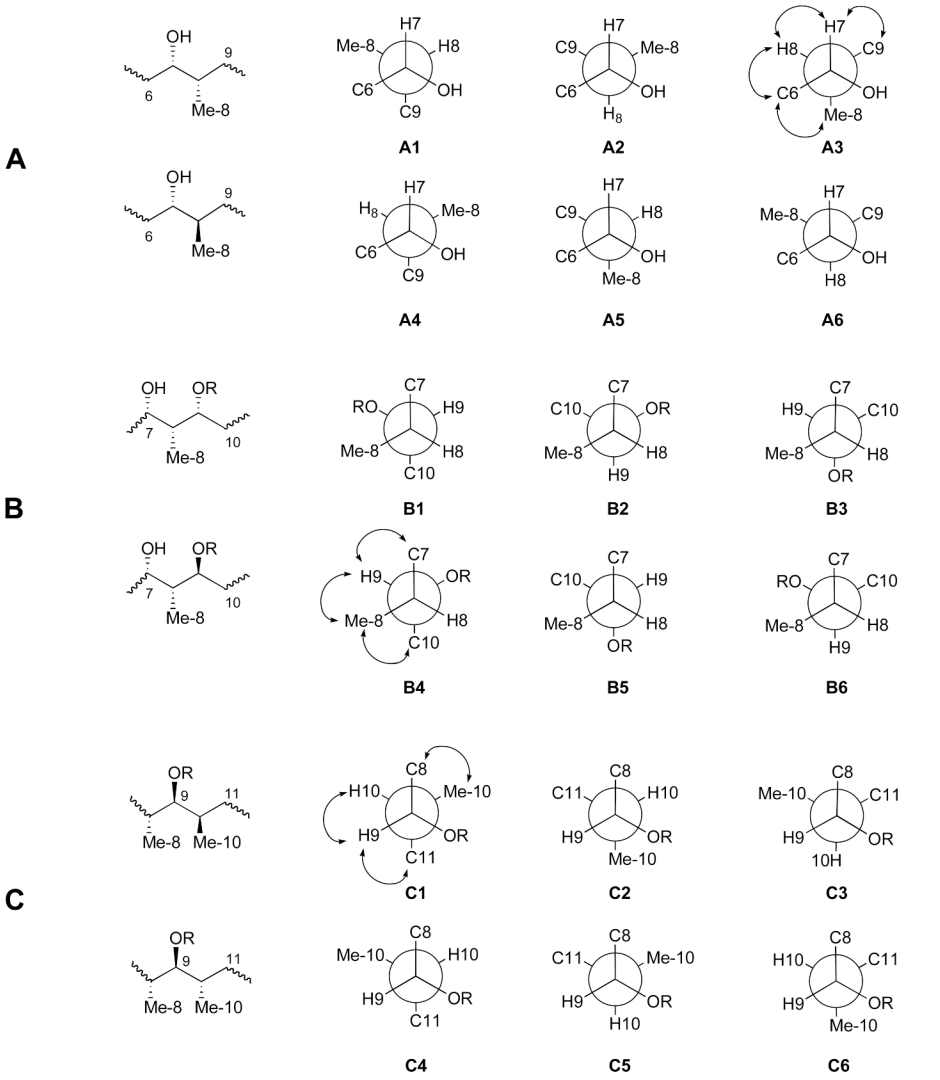

A3	B4	C1
$^{3}J_{H7\text{-}H8}$ = 1.0 Hz	$^{3}J_{H8\text{-}H9}$ = 10.6 Hz	$^{3}J_{H9\text{-}H10}$ = 1.1 Hz
$^{3}J_{H7\text{-}C9}$ = 3.1 Hz[a]	$^{3}J_{H9\text{-}C7}$ = 3.0 Hz[a]	$^{3}J_{H9\text{-}C11}$ = 4.0 Hz[c]
$^{3}J_{H8\text{-}C6}$ = 2.6 Hz[a]	$^{3}J_{Me8\text{-}H9}$ = 1.3 Hz[b]	$^{3}J_{Me10\text{-}H9}$ = 5.3 Hz[c]
$^{3}J_{Me8\text{-}H7}$ = 5.5 Hz[a]	$^{2}J_{C9\text{-}H8}$ = -7.2 Hz[b]	$^{2}J_{C9\text{-}H10}$ = 1.3 Hz[b]

[a] *J*-HMBC, [b] HETLOC, [c] HSQMBC

Figure 1.

Newman projections showing all possible staggered rotamers for *threo* and *erythro* configurations viewed down bonds (A) C7-C8, (B) C8-C9, and (C) C9-C10 for the polyketide residue Ddtd in compound **1**. $^{3}J_{H\text{-}H}$ and $^{2,3}J_{C\text{-}H}$ values that led to the assignment of the rotamers **A3**, **B4**, and **C1** are displayed. Observed ROEs are shown as double-sided arrows.

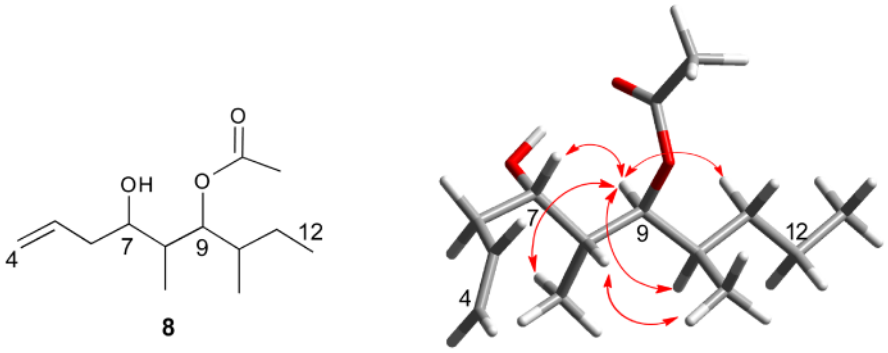

Figure 2.
Chemical structure of **8**, representative of the C-4 to C-12 fragment of Ddtd in **1**-**3**, and DFT mPW1PW91/6-31G(d,p) geometry and energy optimized conformer. Observed ROEs are indicated with double sided red arrows.

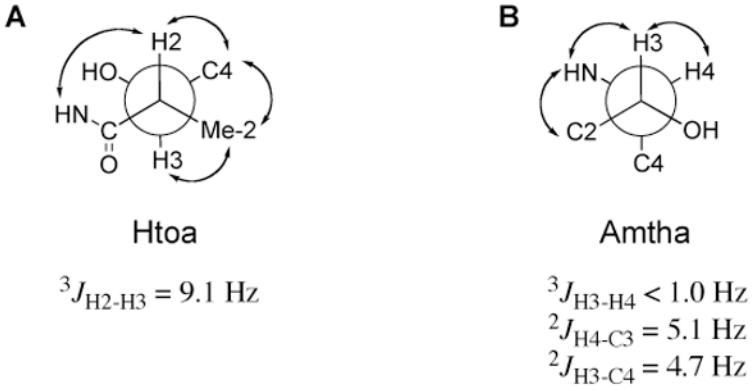

Figure 3.
Newman projections, $^3J_{H-H}$ and $^{2,3}J_{C-H}$ values, and ROESY correlations used to establish the relative configurations of A) C-2/C-3 in Htoa, and B) C-3/C-4 in Amtha.

Table 1

NMR Spectroscopic Data for Celebeside A (**1**) (CD_3CN-D_2O 5:1).

	1			
	δ_C[a]	**δ_H[b] (*J* in Hz)**	**HMBC[c]**	**ROESY[d]**
		Iser		
1	174.9			
2	70.4	4.25 dd (7.8, 3.1)	1. 3	3a, 1_{Thr}
3a	43.9	3.55 m	1, 2, 1_{Ddtd}	NH
3b		3.41 m	1, 2, 1_{Ddtd}	NH
NH		7.98 br t (5.3)		2, 3, 2_{Ddtd}, 3_{Ddtd}
		3-CThr		
1	171.2			
2	57.7	4.62 dd (8.0, 4.5)	1, 3, 4, 1_{Iser}	3, 4, NH, $NH_{\beta MeAsn}$
3	71.0	5.01 m	1, 2, 4, $CO_{Carbamic\ acid.}$	2, 4
Me-3	16.9	1.17 d (6.4)	2, 3	2, 4
4	157.8			
NH_2-4		Na		
NH		8.02 d (8.0)		2, 3, 4, 2_{Iser}
		βMeAsn		
1	171.6			
2	56.3	4.47 dd (8.2, 5.1)	1, 3, 4, βMe, 1_{Thr}	3, βMe, NH, NH_{Ser}
3	41.0	3.09 m	2, 4, βMe	2, βMe, NH_2-4
4	178.9			
βMe	15.5	1.10 d (7.1)	2, 3, 4	2, 3, NH, NH_2-4
NH		8.14 (8.2)		1, βMe, 2_{Thr}, 3_{Thr}
NH_2-4		6.68		3
		7.26		3, βMe
		pSer		
1	171.2			
2	51.4	4.92 m	1, 3, $1_{\beta MeAsn}$	3, NH, NMe_{NMeVal}
3[a]	65.2	3.95 dd (9.6, 18.0)	1, 2	2, NH, 3_{Ddtd}, 4_{Ddtd}, 5_{Ddtd}
3b		3.85 m	1	2, NH, 3_{Ddtd}, 4_{Ddtd}, 5_{Ddtd}
NH		7.85 d (4.6)		2, 3, $2_{\beta MeAsn}$
		*N*MeVal		
1	171.3			
2	63.0	4.70 d (10.7)	1, 4, 5, NMe, 1_{Pser}	4, 5, NMe, 7_{Ddtd}
3	27.7	2.15 m	1, 2, 4, 5	4, 5, NMe
4	18.7	0.74 d (6.4)	2, 3, 5	2, 3, NMe
5	19.7	0.93 d (6.4)	2, 3, 4	2, 3, NMe
NMe	31.7	3.05 s	2, 1Pser	2, 3, 4, 5, 2_{Ser}
		Ddtd		

1

	δ_C[a]	δ_H[b] (*J* in Hz)	HMBC[c]	ROESY[d]
1	169.5			
2	123.5	6.00 d (15.5)	1, 3, 4, 5	NH_{Iser}
3	141.6	7.06 dd (15.5, 11.1)	1, 2, 4, 5	5, NH_{Iser}
4	131.4	6.23 dd (15.3, 11.1)	2, 3, 5, 6, 7	6, 7, 8, Me-8[e], 3_{Ser}, NMe_{NMeVal}
5	140.2	6.05 dd (15.3, 6.6)	3, 4, 6, 7	6, 7, 8, Me-8[e], 3_{Ser}, NMe_{NMeVal}
6a	38.6	2.34 td (13.9, 6.6)	4, 5, 7, 8	4, 5, 7, Me-8[e]
6b		2.20 td (13.9, 6.6)	4, 5, 7, 8	4, 5, 7, Me-8[e]
7	70.6	3.33 t (7.4)	5, 6, 8, 9, Me-8	4, 5, 6, 8, 9, 2_{NMeVal}
8	38.5	1.70 m	9, Me-8	4, 5, 7, 9, Me-8[e], Me-10[e]
9	78.7	5.00 dd (10.6, 1.1)	6, 7, 10, 11 Me-8, Me-10	7, 8, 10[e], 11[e], Me-8[e]
10	34.3	1.76 m	11, 12, Me-10	9, 12 [e]
11a	37.5	1.18 m	10, 12, Me-10	9[e]
11b		1.08 m	10, 12Me-10	9[e]
12a	21.0	1.30 m	10, 11, 13	9[e], 10[e]
12 b		1.19 m		9[e], 10[e]
13	14.5	0.82 t (7.1)	11, 12	
Me-8	9.00	0.794 d (7.0)	7, 8, 9	7[e], 8[e], 9[e], 10[e]
Me-10	12.9	0.796 d (6.0)	9, 10, 11	8[e], 9[e], 10[e]

[a] Recorded at 500 MHz; referenced to residual CD_3CN at δ 1.93 ppm.

[b] Recorded at 125 MHz; referenced to residual CD_3CN at δ 117.7 ppm.

[c] Proton showing HMBC correlation to indicated carbon (CD_3CN-D_2O 5:1)

[d] Proton showing ROESY correlation to indicated proton (CD_3CN-H_2O 5:1)

[e] ROE correlation obtained from the HSQC-ROESY spectrum (CD_3CN-D_2O 5:1)

Table 2

Calculated and experimental *J* values for a fragment corresponding to Ddtd in celebeside A (**1**).

	Calculated[a]						**Experimental**[b]
	Threo			**Erythro**			
C-7/C-8	A1	A2	**A3**	A4	A5	A6	
H7-Me8	2.7	4.0	4.3	2.9	4.2	5.1	5.5
H7-C9	4.9	0.4	2.1	5.6	1.5	0.1	3.1
H8-C6	4.4	1.7	0.5	0.7	5.2	5.7	2.6
H8-H7	2.7	7.5	2.2	2.4	4.1	6.3	1.0
TAD[c]	*8.0*	*11.7*	***5.5***	*8.4*	*8.7*	*11.8*	
C-8/C-9	B1	B2	B3	**B4**	B5	B6	
H8-C9	-0.4	-4.8	-3.8	-4.1	-0.7	-5.2	-7.2
H9-C7	5.2	5.5	1.8	2.3	2.3	1.2	3.0
H9-Me8	1.5	3.6	2.7	1.0	6.5	5.1	1.3
H9-H8	2.0	2.5	9.0	9.2	1.2	5.1	10.6
TAD	*17.8*	*15.3*	*7.6*	***5.5***	*21.9*	*13.0*	
C-9/C-10	**C1**	C2	C3	C4	C5	C6	
H9-Me10	5.0	0.4	2.5	6.6	4.7	2.9	5.3
H9-C11	2.6	6.2	4.4	0.3	2.2	4.7	4.0
H10-C9	2.3	-2.0	-5.7	-2.1	-5.7	2.3	1.3
H10-H9	2.6	4.4	2.3	4.8	2.3	2.7	1.1
TAD	***4.2***	*13.7*	*11.3*	*12.1*	*10.7*	*5.7*	

[a] *J* values calculated using DFT at the MPW1PW91/6-31G(d,p) level using Gaussian03.[20]

[b] Experimental values derived from HMBC, HETLOC and HSQMBC spectra.

[c] Total Absolute Deviation (TAD) values calculated using the equation ($\Sigma|J_{calc}-J_{exp}|$). Stereoisomers displaying the lowest TAD values appear in bold.

Table 3

Biological activities.

compound	HIV-1 neutralization	HCT-116
1	1.9 ± 0.4	8.8 ± 3.0
3	> 50	> 25
4	0.8 ± 0.3	2.1 ± 0.7
5	nt	4.0 ± 1.7
7	nt	2.1 ± 0.9